AIP | Journal of Renewable and Sustainable Energy

Simple and low cost incremental conductance maximum power point tracking using buck-boost converter

Tey Kok Soon, Saad Mekhilef, and Azadeh Safari

Citation: J. Renewable Sustainable Energy **5**, 023106 (2013); doi: 10.1063/1.4794749

View online: http://dx.doi.org/10.1063/1.4794749

View Table of Contents: http://jrse.aip.org/resource/1/JRSEBH/v5/i2

Published by the American Institute of Physics.

Simple and low cost incremental conductance maximum power point tracking using buck-boost converter

Tey Kok Soon,[1] Saad Mekhilef,[1] and Azadeh Safari[2]
[1]*Department of Electrical Engineering, University of Malaya, 50603 Kuala Lumpur, Malaysia*
[2]*Department of Electronic Engineering, Macquarie University, 2109 Sydney, Australia*

(Received 22 October 2012; accepted 22 February 2013; published online 7 March 2013)

Cost of the photovoltaic (PV) systems and their peripherals has been always an issue when considering them for various applications. Using an inexpensive maximum power point tracking (MPPT) system is a simple but efficient solution to reduce the cost of the PV systems and increase the public acceptance. This paper presents the simulation and hardware implementation of incremental conductance algorithm using buck-boost converter and PIC18F4520 controller. Design and simulation of the proposed system are presented using MATLAB and SIMULINK tools. The proposed system is also tested on KC85T PV module for constant and changing weather conditions. Experimental results indicated the capability and functionality of the proposed system on tracking maximum power point with the voltage ripple ratio = 0.006, which is near to the ideal mathematically calculated assessment. The proposed MPPT system helps to reduce the complexity and cost of the PV systems and also ensures the largest operating region of the PV module. © *2013 American Institute of Physics*. [http://dx.doi.org/10.1063/1.4794749]

I. INTRODUCTION

Traditional electricity generation using thermal energy by burning charcoal and other fossil fuels has become more costly due to the remarkable increase in fuel prices. The thermal generation has also been considered as one of the leading causes for greenhouse gas emissions and global warming.[1–3] Meanwhile, the solar power is considered as one of the solutions to the environmental problems and a promising energy source for generating electricity. Despite all the advantages, electricity generated by the PV module is an extremely unstable power source. The change in sunlight intensity, ambient temperature or load will change the output voltage and power of the PV module significantly. Thus, developing ways to boost the efficiency and advantageous of the PV system is highly concerned.[4]

In order to ensure that the PV module always operates at the maximum power point (MPP) for any weather and temperature conditions, a maximum power point tracking (MPPT) system is indispensable.[5–7] Each operating point of the PV module can be reported by an operating current and operating voltage. So, when the PV module is operating at the MPP current and voltage, it generates the maximum power available. Maximum power point of a PV module is always fluctuating in an interval depending on the cell type, irradiation, and cell temperature. Hence, the main role of the MPPT is to operate the PV system at its maximum power point under given temperature and irradiance.[8]

Various MPPT methods have been developed and implemented in the literature. They vary in complexity, sensors required, convergence speed, cost, range of effectiveness, hardware implementation, and popularity.[9] Some of the most popular MPPT methods are incremental conductance, perturbation and observation (P&O), fractional open-circuit voltage (FOCV), fractional short-circuit current (FSCC), and fuzzy logic control (FLC).[6–11] Among these MPPT methods, incremental conductance method offers a good performance under quick changes in weather conditions. Besides, it is also simple and can be implemented using low cost microcontroller.[6,9]

In this paper, incremental conductance method is used. A low cost programmable integrated circuit (PIC) controller has been employed to control the switching activity of a buck-boost

converter. Generally, simple converters such as buck and boost are used for existing MPPTs in the literature; however, their operational region is small compared to the buck-boost converter which has the capability to step up and step down the input voltage.[11–14] In addition, PIC controller has merits over a digital signal processor (DSP) microcontroller since it is cheaper and its controlling program is simple.[13–16]

II. PV MODULE CHARACTERISTICS

The basic structure of a PV system is the PV module, which is composed of solar cells. A solar cell converts energy in the photons of sunlight into electricity by means of the photovoltaic effect found in certain types of semiconductor materials, such as silicon and selenium. An individual solar cell can only produce a small amount of power. A PV module is a current source composed of parallelly and serially connected PV cells.[13,17,18] To increase the electrical output power of a system, PV modules are usually connected in series or parallel to form a PV system.[19] Using the Kirchhoff's current law (KLC) in the PV equivalent electric circuit, the current produce by a PV module is[20,21]

$$I = n_p I_{SC} - n_p I_O * \{\exp[q(V/n_s + R_S I)/nkT_k] - 1\} - (V + R_S I)/R_{sh}, \quad (1)$$

where V is the output voltage of PV module, I output current of PV module, R_s series resistance of cell, R_{sh} shunt resistance of cell, q, electronic charge (1.602×10^{-19} C), I_{sc} light-generated current, k, Boltzman constant (1.38×10^{-3} J/k), T_k temperature (K), n_s number of PV cells connected in series, n_p number of PV cells connected in parallel, and I_o the reverse saturation current which depends on the ambient temperature

$$I_o = I_{sc} \cdot \left(e^{\frac{qVoc}{nKT}} - 1\right). \quad (2)$$

Equation (1) shows that the PV module output power is affected by two weather variables which are the solar irradiation and the temperature.

To investigate the effects of temperature and solar irradiation on the output power of PV module, two main characteristic curves of the PV module are considered: the current vs. voltage curve (I-V curve) and the power vs. voltage curve (P-V curve). Fig. 1 shows the I-V and P-V characteristic curves of a PV module.[23,24] Three points on the P-V curve are important in defining the performance of a PV module: the maximum power point, the short-circuit current, and the open-circuit voltage.[22]

The PV module can be operated in any point on the I-V curve between the I_{sc} and the V_{oc}. However, the power from the PV module is different in every operating point as shown in the

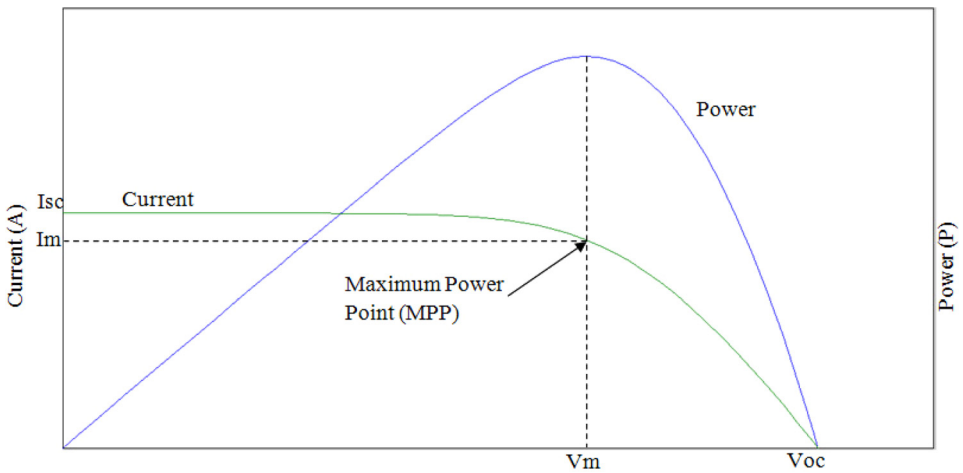

FIG. 1. I-V and P-V characteristic curves of a PV module.

P-V curve in Fig. 1. Therefore, a control algorithm is needed in order to ensure that the PV system always operates at the MPP.

Fig. 1 is obtained when the temperature and solar irradiation are constant at the standard testing conditions (STC) which are defined as cell temperature = 25 °C, incident solar irradiance = 1000 W/m^2, and air mass (AM) = 1.5.

III. MPPT ALGORITHMS

Many MPPT algorithms have been proposed to track the MPP. Some of the proposed MPPT algorithms are simple such as voltage and current feedback based methods and some are more complicated such as P&O or the incremental conductance method. They also vary in complexity, sensor requirement, speed of convergence, cost, range of operation, popularity, ability to detect multiple local maxima, and their applications.[25] In the following, two common algorithms are discussed.

A. P&O method

P&O method is the most commonly used MPPT method in the literature.[26–31] It is based on the output power of the PV module. When the output power is increased due to the increase in the output voltage, the voltage will keep increasing until MPP is reached. When the output power is decreasing, the voltage will be tuned back again. This process will keep going to ensure that the PV module operates at the MPP.[17,32]

P&O algorithm is simple and efficient; however, there are downsides since it cannot always keep the PV system at the MPP due to the slow trial and error process. Using P&O algorithm even for steady-state sunshine keeps the PV system in an oscillating mode and hence the output is fluctuating and finally the operation of the PV system may fail to track the MPP due to the sudden changes in solar irradiation level.[32]

B. Incremental conductance method

This algorithm uses the instantaneous conductance of the PV module which is the current divided by the voltage $\left(\frac{\mathrm{I}}{\mathrm{V}}\right)$ and the incremental conductance which is the difference of current divided by the difference of voltage $\left(\frac{\Delta \mathrm{I}}{\Delta \mathrm{V}}\right)$ and compares them in order to obtain the MPP. Graphically, this method depends on the P-V curve characteristics of the PV module. Equations (3)–(5) are used in incremental conductance method to determine the operating point of the PV module[23,33]

$$\frac{\Delta I}{\Delta V} = \frac{I}{V}, \tag{3}$$

$$\frac{\Delta I}{\Delta V} > -\frac{I}{V}, \tag{4}$$

$$\frac{\Delta I}{\Delta V} < -\frac{I}{V}. \tag{5}$$

Equation (3) is held true when the PV module is operating at the MPP; Eq. (4) is held true when the PV module is operating in the left region of the MPP in the P-V curve; and Eq. (5) is held true when the PV module is operating in the right region of the MPP in the P-V curve. This algorithm is based on the fact that the gradient of the P-V curve is equal to zero at MPP[33]

$$\frac{dP}{dV} = 0. \tag{6}$$

Since,

$$\frac{dP}{dV} = I\left(\frac{dV}{dV}\right) + V\left(\frac{dI}{dV}\right), \tag{7}$$

$$\frac{dP}{dV} = I + V\left(\frac{dI}{dV}\right), \tag{8}$$

using (6), Eq. (8) can be derived as

$$I + V\left(\frac{dI}{dV}\right) = 0. \tag{9}$$

However, condition in (9) is difficult to be obtained and therefore, there is a small permitted error.[33] Equation (9) can be rewritten as

$$\left|I + V\left(\frac{dI}{dV}\right)\right| = e, \tag{10}$$

where e is the small permitted error and a small positive number.

The main advantage of this algorithm is its fast power tracking process but it might be unstable when the solar intensity is low due to the low current differentiation. The flow chart of incremental conductance algorithm is shown in Fig. 2.

In this paper, incremental conductance method is used as the MPPT algorithm; advantages of using this method are the higher efficiency, accuracy, and fast tracking of MPP in comparison with other algorithms.

IV. SELECTING A PROPER DC-DC CONVERTER

MPPT system is simply a DC-DC converter, which acts as a power interface between the PV module and the load. The key characteristic in designing a MPPT is to control the switching activity of the converter and deliver the maximum power to the load at each operating condition. When a PV module is connected to a load, its operation point will be determined by the intersection point of its I-V curve and the load line. At a single point, when two curves intersect each other exactly at the MPP, the PV module is operating at the MPP.[14] There are several non-isolating DC-DC converters, including buck, boost, buck-boost, SEPIC, and Cuk converters. Among all these converters, the buck-boost converter has a simple structure and a lower cost compared to the other converters. It can also be operated in continuous and discontinuous inductor current modes. In this paper, the buck-boost converter is used to operate in the continuous current mode. Therefore, in the following, only continuous current mode will be discussed. Continuous inductor current mode is characterized by current flowing continuously in the inductor during the entire switching cycle in steady-state condition.[34] During the operation time, the switching activity of buck-boost converter is controlled by the Pulse-Width Modulation (PWM) in order to control the operation mode of the converter. The relationship between the input and the output voltage of the buck-boost converter is

$$V_{out} = -V_{in}\frac{D}{1-D}. \tag{11}$$

When the converter is in ideal condition, the input power is equal to the output power as

$$P_{in} = P_{out}, \tag{12}$$

$$V_{in}I_{in} = V_{out}I_{out}. \tag{13}$$

By substituting (11) into (13)

$$I_{out} = -I_{in}\frac{1-D}{D} \tag{14}$$

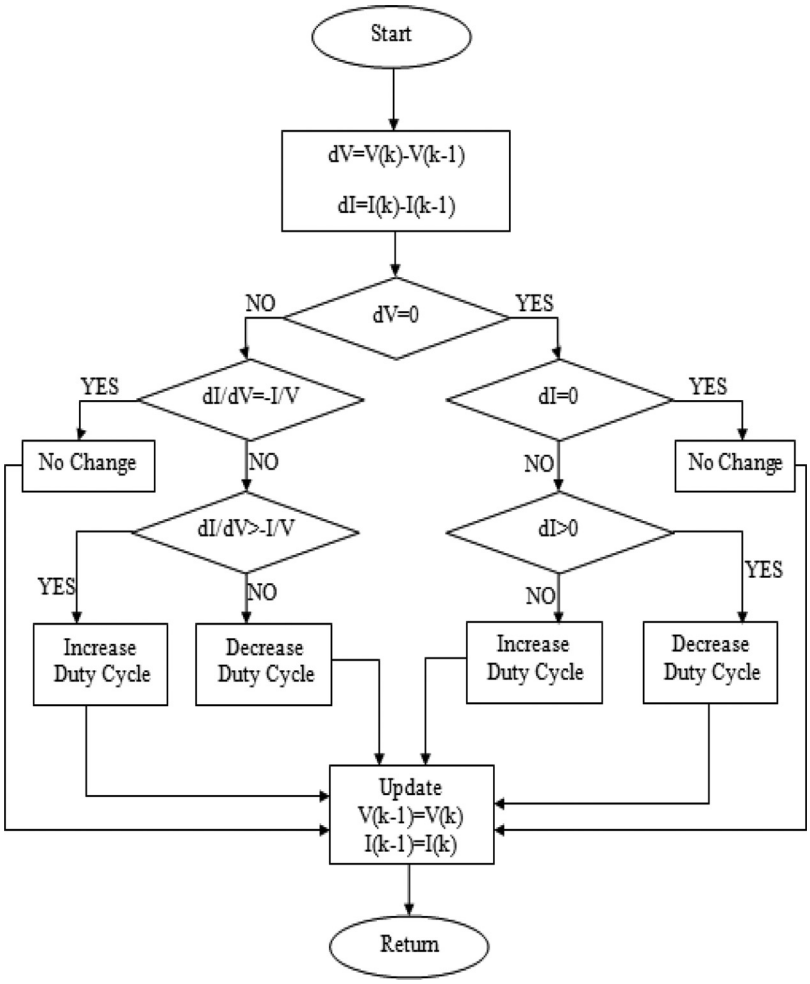

FIG. 2. Flowchart of incremental conductance (IC) method.

and dividing (11) with (14) result in

$$\frac{V_{out}}{I_{out}} = \frac{V_{in}}{I_{in}} \frac{D^2}{(1-D)^2}, \tag{15}$$

$$R_{in} = R_{out} D'', \tag{16}$$

where $D'' = \frac{(1-D)^2}{D^2}$.

Equation (16) shows that the input impedance of the converter can be adjusted by changing the duty cycle of the converter. Since the load line of the system can be adjusted by changing the input impedance of the converter,[35] the load line is moved to ensure that the PV module operates at the MPP. The ripple ratio and the L_{min} are calculated using

$$\frac{\Delta V_o}{V_o} = \frac{DT}{RC} = \frac{D}{RCf}, \tag{17}$$

$$L_{min} = \frac{R}{2f}(1-D)^2. \tag{18}$$

The operating region of buck-boost converter can be studied by imposing the load line onto the I-V curve. The inclination angle of the load line for buck-boost converter can be expressed as[14]

$$\Theta_{Rin} = \tan^{-1}\left[\frac{D^2}{(1-D)^2 R_{out}}\right]. \quad (19)$$

Using this equation, comparing the operational and non-operational regions of buck-boost, buck, and boost converters shows the wider operation region for buck-boost converter. Buck-boost converter has no non-operational region because the input voltage can be either step up or step down. However, buck and boost converters can only step down or step up the input voltage. Hence, the operational region of the buck-boost converter is the combination of the operational region of both the buck and the boost converters.

V. SYSTEM DESIGN AND SIMULATION

The DC-DC converter has been designed and simulated using MATLAB and SIMULINK tools. The capacitor has direct effect on the output voltage ripple. It should be large in order to ensure the smallest ripple in the output voltage. By substituting the capacitance value 1000 μF in Eq. (17), the ripple ratio is 0.008. The switching frequency of the converter is set to 10 kHz and the load is chosen to be a 10 Ω power resistor. Substituting the minimum duty cycle D = 0.2 in Eq. (18), the minimum inductor is calculated to be $L_{min} = 320\ \mu$H.

In the simulations, the PV module has been modeled as well. In this paper, KC85T with specifications as shown in Table I is used for simulations and hardware implementation.

First, the PV module model is tested at the constant reference temperature 25 °C while the solar irradiation level is increasing from 600 W/m^2 to 1000 W/m^2 at 0.1 s. When the solar intensity is at 1000 W/m^2, the PV module is operating at STC and the voltage and current of PV module at MPP are as stated in Table I. By substituting the voltage and current to Eq. (15), the duty cycle at MPP is calculated, D = 0.63.

The output voltage during steady state is around 9.4 V between 0 s and 0.1 s. When the irradiation level changes to 1000 W/m^2 at 0.1 s, the voltage starts to increase slowly and reaches to the steady state condition at 14.27 V. The ripple for the steady state waveform is about 0.09 V and the ripple ratio $\frac{\Delta V_o}{V_o} = \frac{0.09}{14.2}$ is about 0.006 which is near to the ideal mathematically calculated value, 0.008.

The inductor current is used as the maximum operating current for the DC-DC converter. The current waveforms of the inductor and diode show that the converter operates at the continuous mode with current equal to 4.8 A.

VI. HARDWARE IMPLEMENTATION

The proposed system consists of the PV module, DC-DC converter, PIC controller, PWM, and the load. By controlling the duty cycle of the DC-DC converter, the operating point of the PV module is moved to the MPP. PIC controller is programmed with incremental conductance algorithm to generate the suitable PWM which is used to control the duty cycle. The current of the PV module is sensed by the current sensor from LEM, LTS 15-NP. A voltage divider is designed to sense the input and output voltage of the converter. The output terminal of the converter is connected to a constant load.

The hardware implementation of buck-boost converter is shown in Fig. 3. Each part is marked on the figure and the description of each part is provided in Table II.

TABLE I. PV module's parameters (KC85T module).

Maximum power (P_{max})	87 W
Voltage at MPP (V_{mpp})	17.4 V
Current at MPP (I_{mpp})	5.02 A
Open circuit voltage (V_{oc})	21.7 V
Short circuit current (I_{sc})	5.34 A

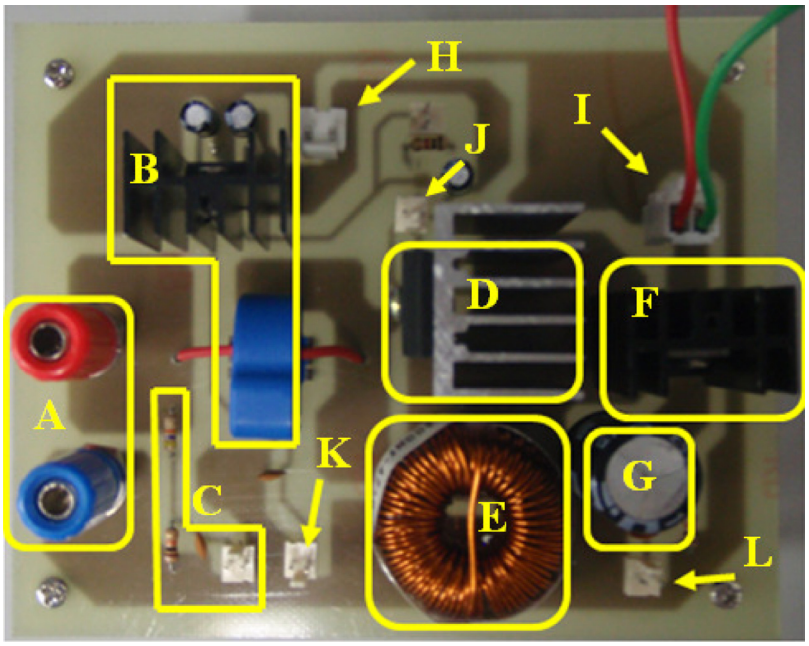

FIG. 3. Buck-boost converter.

VII. CONTROL CIRCUIT CONFIGURATION

In order to always exploit the maximum power from the PV module, the incremental conductance algorithm is coded into a PIC controller. The controller uses the input current and voltage of the converter to calculate the suitable PWM for the IGBT. The PWM signal from the controller is amplified from 5 V to 15 V by using a gate drive circuit since the IGBT operates with 12 V signal.

In this paper, the PIC18F4520 from Microchip is used with frequency range between 32 kHz and 40 MHz. The processing speed depends on the connection of the external clock

TABLE II. Components specifications of the hardware implementation.

Part	Description
A	Input port of the converter (Blue terminal is the ground) Connected to the PV module output terminals
B	Current sensor IC 7805 is used to supply 5 V to the LEM current sensor
C	Voltage divider consist of 47 kΩ and 10 kΩ resistors The voltage across the 10 kΩ resistor is measured with respect to the ground
D	IGBT switch with heat sink N-Channel IGBT, FGH50N6S2, 100 kHz operating at 390 V and 40 A
E	490 μH power inductor with maximum 5.0 A current rating
F	Switch mode power diode, MBR1080, rating 10 A and 80–100 V
G	1000 μF capacitor with voltage rating 50 V
H	12 V input port
I	Output terminal of the converter connected to the 100 W, 10 Ω power resistor
J	Input port connected to the gate drive circuit Gate drive will control the switching activity of the IGBT
K	Output port sends the signal from the LEM current sensor to the PIC controller
L	Output port of the voltage divider senses the output voltage of the converter

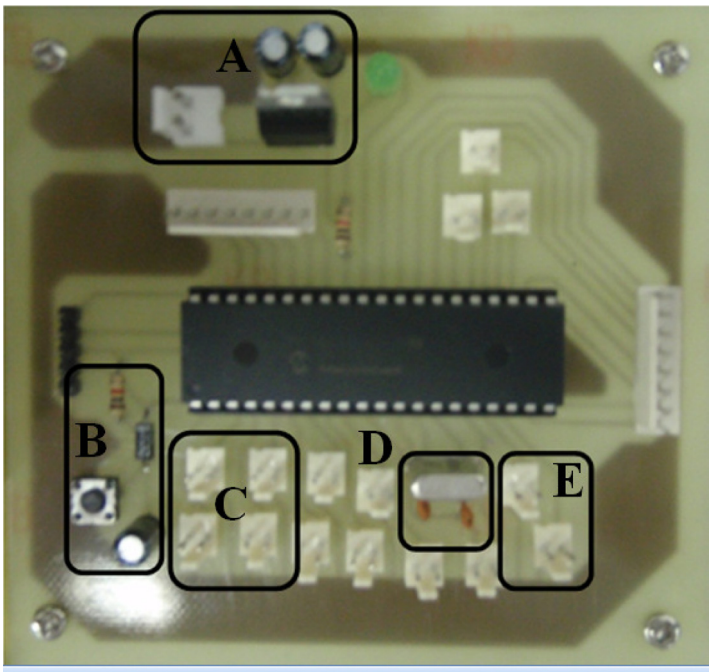

FIG. 4. Hardware implementation of PIC Controller (PIC18F4520) board.

generator circuit and the high speed crystal/resonator with phase-locked loop (PLL) enabled mode is used to produce the 40 MHz clock pulse. A 10 MHz crystal and two 15 pF capacitors are used to generate the clock pulse.

Fig. 4 shows the hardware implementation of the PIC controller. Each component on the controller board is marked and Table III describes the component specifications.

Employing PIC controller has many advantages including cost efficiency of less than $50, easy to programming and debugging, and large range of interfaces. They have also built-in oscillator with selectable speeds. They use 10-bit analog to digital converter (ADC) and processing speed of 40 MHz which is appropriate for MPPT system. They can also provide the required frequency to generate the PWM signal. In summary, PIC is capable of taking control of the MPPT system with less cost and complexity compared to DSP.

Another approach in this paper is that by applying buck-boost converter, the PV module operates in a larger operational region. The structure of this converter is also simpler and easier to build than that of other types of DC-DC converters. Buck-boost converter also provides an output voltage polarity reversal without a transformer. It has high efficiency, current limiting and the output short circuit protection is easy to implement.

TABLE III. Description of hardware design of PIC controller.

Part	Description
A	IC 7805 is used to converter 12 V input to 5 V and supply the 5 V to the PIC
B	Master clear circuit of the PIC controller Used to reset the PIC controller
C	Analog to digital converter (ADC) input pin The signal from LEM current sensor and voltage divider goes to this input
D	The crystal connection of the PIC controller
E	Output port which sends the PWM signal to the gate drive circuit

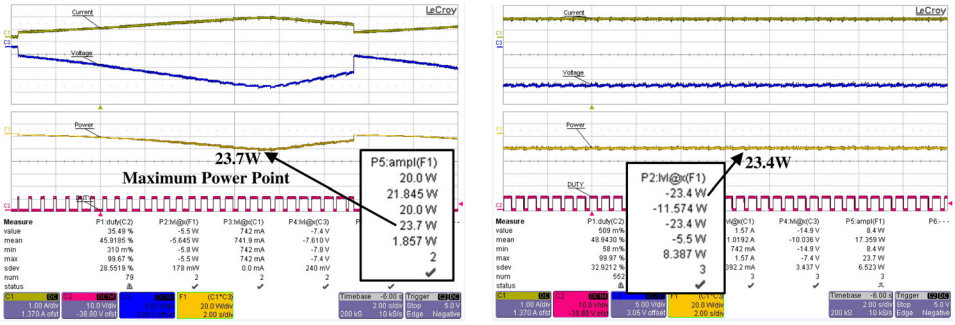

FIG. 5. Output waveforms: (a) The duty cycle increased from 0.2 to 0.8 to obtain the MPP. (b) MPPT is implemented.

VIII. RESULTS AND DISCUSSIONS

Two PV modules are connected in parallel for testing the functionality of the proposed MPPT system. The proposed system is tested in constant and changing weather conditions.

First, the performance of the proposed MPPT is studied under constant weather conditions and the output current, voltage and power of the PV module without and with MPPT have been observed. When the duty cycle is increased from 0.2 to 0.8, the output power has been increased slowly until the maximum power point is reached and then it decreased. By this way, the P-V curve of the PV module is obtained. The waveforms are shown in Fig. 5(a). From the P-V curve, the MPP is obtained and then the MPPT algorithm is run and the result of the output waveform is shown in Fig. 5(b). By comparing both of the figures, it is obvious that the MPP obtained by the MPPT algorithm is matched with the MPP of the PV module.

For testing the performance of the proposed system in different irradiation levels, numbers of the PV modules are increased from one to two modules and the change in the current, voltage and power is observed. Fig. 6 shows the output current, voltage and power of the PV module. The output power for one PV module is 20 W. A PV module is then added using parallel connection and the output power increased to 40 W. The output power returns back to 20 W when the second PV module is disconnected. The same trend is happening for output current and voltage of the PV module. This test has been performed under real conditions and hence the output current and voltage are not same as the ones at STC.

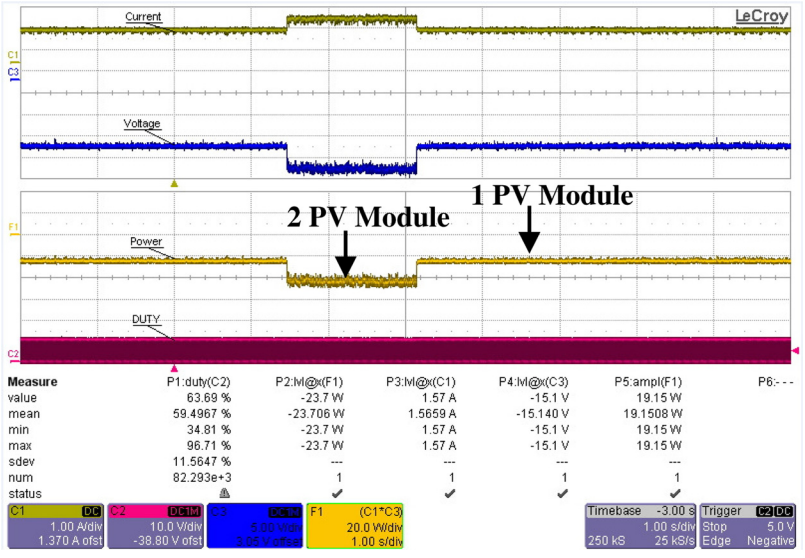

FIG. 6. Output current (upper), voltage (middle), and power (lower) waveforms of 1 and 2 PV modules.

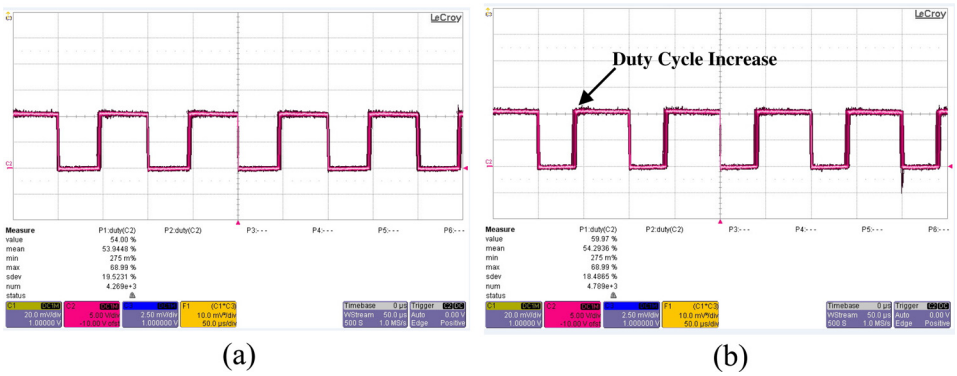

FIG. 7. Change in the duty cycle due to change in number of PV modules. (a) One PV module. (b) Two PV modules.

The change in the duty cycle is also observed when the number of the PV module is increased from one to two modules. First, single PV module is connected to the PV system and the PIC controller generates the PWM with duty cycle, $D = 0.54$. By increasing the number of the PV module to two modules, the MPP moves to another location. Hence, the duty cycle is increased to $D = 0.6$ in order to track the new MPP. Fig. 7 shows the results of the changing in duty cycle due to the change in the number of PV modules.

The proposed MPPT has been tested for rapidly changing weather conditions as well. In order to provide the partial and full shadow conditions, the PV module was covered partially and fully, respectively. For the fast moving cloud, the PV module is covered for a short period and the process is repeated for a few times. Fig. 8 shows the drop of the output power when the PV module is in partial shadow condition and no power has been delivered when the PV module is covered with full shadow. Finally, the output power is following the movement of the cloud in the fast moving cloud condition. The PV module produces no output power when there is full shadow. It generates full power when the shadow is passed through.

The resultant waveforms have been measured from the output side of the converter since the input current of the buck-boost converter is in the discontinuous mode. Therefore, the PV module only supplies power to the buck-boost converter when the switch (IGBT) is on. Using Eq. (16),

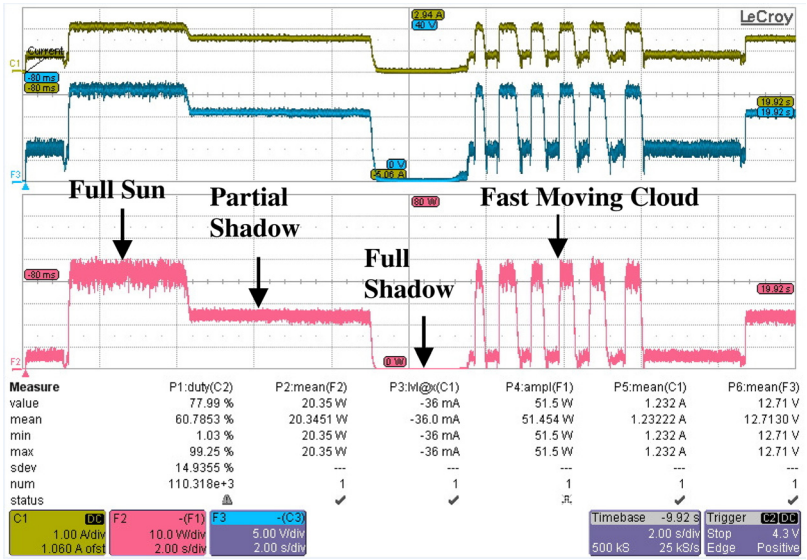

FIG. 8. Output waveforms under varying weather condition.

the duty cycle for solar irradiation levels between 500 W/m^2 and 1000 W/m^2 is 0.5 to 0.63, respectively, which means that the switch of the buck-boost converter is on for about 50% of the operating period. Hence, the average input power is 50% of its normal value. In order to overcome this problem, other types of converters can be used such as Cuk or SEPIC converters which are also able to step up and step down the input voltage with continuous input current.

IX. CONCLUSION

The proposed MPPT system is able to track the MPP under constant and varying weather conditions. Therefore, the objective of this paper is achieved where a low complexity and cost efficient MPPT system is designed, simulated, and implemented. The maximum power has been extracted from the PV module of two parallel KC85T modules. By using a low cost PIC controller to sense the PV module's output voltage and current, duty cycle of the Buck-Boost converter is adjusted to keep the PV system operating at the MPP. The buck-boost converter provided a discontinuous input current and the output voltage is inverted.

ACKNOWLEDGMENTS

The authors would like to acknowledge the HIR-MOHE Project. The research has been carried out under the Project No. UM.C/HIR/MOHE/ENG/24.

[1]S. Mekhilef, R. Saidur, and A. Safari, "A review on solar energy use in industries," Renewable Sustainable Energy Rev. **15**, 1777–1790 (2011).
[2]W. Rong-Jong, W. Wen-Hung, and L. Chung-You, "High-performance stand-alone photovoltaic generation system," IEEE Trans. Ind. Electron. **55**, 240–250 (2008).
[3]S. Mekhilef, A. Safari, W. E. S. Mustaffa, R. Saidur, R. Omar, and M. A. A. Younis, "Solar energy in Malaysia: Current state and prospects," Renewable Sustainable Energy Rev. **16**(1), 386–396 (2012).
[4]W. Liu and Y. Bao, "Research of maximum power point tracking for photovoltaic with buck chopper," in *3rd International Workshop on Intelligent Systems and Applications (ISA)* (IEEE Conference Publications, 2011), pp. 1–4.
[5]See http://www.blueskyenergyinc.com/uploads/pdf/BSE_What_is_MPPT.pdf for the description on the concept of Maximum Power Point Tracking (MPPT).
[6]X. Weidong, A. Elnosh, V. Khadkikar, and H. Zeineldin, "Overview of maximum power point tracking technologies for photovoltaic power systems," in *IECON 2011—37th Annual Conference on IEEE Industrial Electronics Society* (IEEE Conference Publications, 2011), pp. 3900–3905.
[7]K. Ishaque, Z. Salam, M. Amjad, and S. Mekhilef, "An improved particle swarm optimization (PSO) based MPPT for PV with reduced steady state oscillation," IEEE Trans. Power Electron. **27**(8), 3627–3638 (2012).
[8]A. Safari and S. Mekhilef, "Implementation of incremental conductance method with direct control," in *2011 IEEE Region 10 Conference* (IEEE Conference Publications, 2011), pp. 944–948.
[9]T. Esram and P. L. Chapman, "Comparison of photovoltaic array maximum power point tracking techniques," IEEE Trans. Energy Convers. **22**, 439–449 (2007).
[10]M. A. G. de Brito, L. P. Sampaio, G. Luigi, G. A. e Melo, and C. A. Canesin, "Comparative analysis of MPPT techniques for PV applications," in *International Conference on Clean Electrical Power (ICCEP)* (IEEE Conference Publications, 2011), pp. 99–104.
[11]I. Purnama, L. Yu-Kang, and C. Huang-Jen, "A fuzzy control maximum power point tracking photovoltaic system," in *IEEE International Conference on Fuzzy Systems (FUZZ)* (IEEE Conference Publications, 2011), pp. 2432–2439.
[12]T. Mrabti, M. El Ouariachi, B. Tidhaf, K. Kassmi, and E. Chadli, "Regulation of electric power of photovoltaic generators with DC-DC converter (buck type) and MPPT command," in *International Conference on Multimedia Computing and Systems* (IEEE Conference Publications, 2009), pp. 322–326.
[13]A. Thenkani and N. Senthil Kumar, "Design of optimum maximum power point tracking algorithm for solar panel," in *International Conference on Computer, Communication and Electrical Technology (ICCCET)* (IEEE Conference Publications, 2011), pp. 370–375.
[14]R. F. Coelho, F. Concer, and D. C. Martins, "A study of the basic DC-DC converters applied in maximum power point tracking," in *Power Electronics Conference* (IEEE Conference Publications, 2009), pp. 673–678.
[15]S. Patel and W. Shireen, "Fast converging digital MPPT control for photovoltaic (PV) applications," in *2011 IEEE Power and Energy Society General Meeting* (IEEE Conference Publications, 2011), pp. 1–6.
[16]T.-P. Lee, S.-T. Wu, J.-M. Wang, H.-J. Chiu, and Y.-K. Lo, "A modular PV charger with maximum power point tracking and pulse-charging schemes," in *5th IET International Conference on Power Electronics, Machines and Drives (PEMD 2010)* (IET Conference Publications, 2010), pp. 1–6.
[17]C. Roshau, S. Yuvarajan, and D. Schulz, "Modeling and hardware implementation of VMPPT for a PV panel with a reference cell," in *34th IEEE Photovoltaic Specialists Conference (PVSC)* (IEEE Conference Publications, 2009), pp. 001034–001037.
[18]See http://photovoltaics.sandia.gov/docs/PVFEffIntroduction.htm for the introduction on various types of PV system.
[19]L. Fangrui, D. Shanxu, L. Fei, L. Bangyin, and K. Yong, "A variable step size INC MPPT method for PV systems," IEEE Trans. Ind. Electron. **55**, 2622–2628 (2008).
[20]A. Kassem and M. Hamad, "A microcontroller-based multi-function solar tracking system," in *IEEE International Systems Conference (SysCon)* (IEEE Conference Publications, 2011), pp. 13–16.

[21]M. I. Khan, M. R. Islam, M. Z. Mozumder, and K. M. Rahman, "Photovoltaic maximum power point tracking battery charge controller," in *1st International Conference on the Developments in Renewable Energy Technology (ICDRET)* (IEEE Conference Publications, 2009), pp. 1–5.
[22]F. M. González-Longatt, "Model of photovoltaic module in Matlab," II CIBELEC (2005), pp. 1–5.
[23]C. Bo-Chiau and L. Chun-Liang, "Implementation of maximum-power-point-tracker for photovoltaic arrays," in *6th IEEE Conference on Industrial Electronics and Applications (ICIEA)* (IEEE Conference Publications, 2011), pp. 1621–1626.
[24]See http://www.docstoc.com/docs/20108218/Experiment-1-Solar-Powerand-I-V-Characteristics for the description on the relationship between the load and the I-V curve.
[25]R. Faranda, S. Leva, and V. Maugeri, "MPPT techniques for PV systems: Energetic and cost comparison," in *Power and Energy Society General Meeting - Conversion and Delivery of Electrical Energy in the 21st Century* (IEEE Conference Publications, 2008), pp. 1–6.
[26]H. Chihchiang, L. Jongrong, and S. Chihming, "Implementation of a DSP-controlled photovoltaic system with peak power tracking," IEEE Trans. Ind. Electron. **45**, 99–107 (1998).
[27]T. Noguchi, S. Togashi, and R. Nakamoto, "Short-current pulse-based maximum-power-point tracking method for multiple photovoltaic-and-converter module system," IEEE Trans. Ind. Electron. **49**, 217–223 (2002).
[28]N. Mutoh, M. Ohno, and T. Inoue, "A method for MPPT control while searching for parameters corresponding to weather conditions for PV generation systems," in *30th Annual Conference of IEEE Industrial Electronics Society*, Vol. 3 (IEEE Conference Publications, 2004), pp. 3094–3099.
[29]N. Femia, G. Petrone, G. Spagnuolo, and M. Vitelli, "Optimization of perturb and observe maximum power point tracking method," IEEE Trans. Power Electron. **20**, 963–973 (2005).
[30]N. Fermia, D. Granozio, G. Petrone, and M. Vitelli, "Predictive & adaptive MPPT perturb and observe method," IEEE Trans. Aerosp. Electron. Syst. **43**, 934–950 (2007).
[31]E. Koutroulis, K. Kalaitzakis, and N. C. Voulgaris, "Development of a microcontroller-based, photovoltaic maximum power point tracking control system," IEEE Trans. Power Electron. **16**, 46–54 (2001).
[32]C. Liu, B. Wu, and R. Cheung, "Advanced algorithm for MPPT control of photovoltaic systems," in *Canadian Solar Buildings Conference Montreal* (Solar Buildings Research Network, 2004).
[33]A. Safari and S. Mekhilef, "Simulation and hardware implementation of incremental conductance MPPT with direct control method using Cuk converter," IEEE Trans. Ind. Electron. **58**, 1154–1161 (2011).
[34]See http://focus.ti.com/lit/an/slva059a/slva059a.pdf for the understanding of Buck-Boost Converter.
[35]H. Ying-Tung and C. China-Hong, "Maximum power tracking for photovoltaic power system," in *Industry Applications Conference* (IEEE Conference Publications, 2002), pp. 1035–1040.